

## Computation of refraction static corrections using first-break traveltimes differences

Don C. Lawton\*

### ABSTRACT

Differences in first-arrival traveltimes between adjacent records in multifold reflection surveys can be used to compute the depth and velocity structure of near-surface layers. The procedure uses the redundancy of first-break data in multifold surveys to enable a statistically reliable refraction analysis to be undertaken for either end-on or split-spread recording geometries. The traveltimes differences as a function of source-receiver offset provide a direct indication of the number of refractors present, with each refractor being defined by an offset range with a constant time difference. For each refractor, the time-difference value at a common receiver from two shotpoints is used to partition the intercept time into the delay time at each shotpoint. This procedure is repeated until the delay times at all shotpoints and for all refractors have been computed. Refractor depths and velocities are evaluated from this suite of delay times. A surface-consistent static correction to a selected datum level is then calculated at each surface station, using a replacement velocity equal to that of the deepest refractor.

In a case history from the Canadian Rocky Mountain foothills, short- and intermediate-wavelength weathering static anomalies were resolved successfully. Elevation and weathering static corrections of up to 40 ms were computed, with an estimated error of less than  $\pm 3$  ms.

### INTRODUCTION

In recent years, there has been renewed interest in using the traveltimes of critically refracted seismic energy ("first breaks") to compute weathering static corrections during the processing of reflection seismic data. Automatic residual static methods perform best if refraction static corrections

have been applied first, since correlation across a common-midpoint (CMP) gather depends on the quality of the pilot stacked trace. Furthermore, residual statics alone fail to resolve intermediate- and long-wavelength weathering static anomalies.

In this paper, a procedure is developed for the analysis of refraction data from records acquired during multifold reflection surveys. The technique used is based on delay-time analysis (Gardner, 1967) and is an extension of the reciprocal method published by Hawkins (1961). It also uses the concept of differential shot statics, discussed by Hollingshead and Slater (1979) and Chun and Jacewitz (1981). In my procedure, the multiplicity of first-break data available in multifold reflection surveys is used to determine the number of refractors present and to calculate statistically robust delay times and refractor velocities. Operator input is minimized, yet all possible first-break data are used in the analysis. An important feature is that reciprocal records are not required, thus making the procedure applicable for seismic surveys recorded with an end-on shot configuration. For split-spread data, the analysis can be performed by treating the leading and trailing halves of the records separately. This provides a further statistical confidence test for the analysis.

Conventional analysis of first-break data from end-on records makes use of intercept times and inverse slopes of the refracted-arrival segments of traveltimes-distance graphs to interpret the depth and velocity structure of the shallow subsurface (Gardner, 1939). However, the reliability of this approach can be hampered in the presence of topography or structure on the refractor, which creates ambiguity in the interpretation with respect to the number of refractors present and their true velocities. Cunningham (1974) examined first-break data from end-on records and used differential common-offset traveltimes to fabricate synthetic reverse profiles.

Recently, refraction interpretation based on inversion methods has become popular, particularly ray tracing and generalized linear inversion (Hampson and Russell, 1984). In

Manuscript received by the Editor July 14, 1988; revised manuscript received February 13, 1989.

\*Department of Geology and Geophysics, University of Calgary, 2500 University Drive N.W., Calgary, Alta., Canada T2N 1N4.  
© 1989 Society of Exploration Geophysicists. All rights reserved.

this approach, an input model is designed and theoretical first-break traveltimes are computed. The model is then perturbed iteratively until the computed and observed traveltimes match according to some squared-error criterion. Reliability of inversion schemes depends primarily on the sophistication of the modeling program and the constraints imposed upon the possible solutions.

**THE PROCEDURE**

**Determining the number of refractors**

The integrity of all refraction interpretation methods depends on using first-break data which have been derived from a common refractor. On a first-break traveltime-distance graph, a change in refractor is usually identified by a change in slope at a position called the crossover point (Sheriff, 1984). The identification of true crossover points is difficult if the refractors are not parallel to the ground surface. For example, Figure 1a shows a first-break traveltime-distance plot with two apparent crossovers, for which there are two general solutions, as shown in Figures 1b and 1c. The topography is assumed to be flat along the recording spread. In both interpretations, segment (I) of the graph in Figure 1a represents the direct arrival in the first layer. Figure 1b is a simple, three-layered interpretation in which segments (II) and (III) of the traveltime-distance curve represent arrivals from two successively deeper refractors, with actual velocities given by their respective reciprocal

slopes. Figure 1c is a two-layered solution, where traveltime segments (II) and (III) represent apparent downdip and updip refractor velocities, respectively. The interpretation would have been complicated further if there had been surface topography as well.

The number of refractors present can be determined explicitly by examining the differences between first-arrival traveltimes on records from overlapping spreads. Figure 2a shows first-break traveltime-distance graphs for two adjacent end-on records with shotpoints  $sp_1$  and  $sp_2$ . These graphs could also be viewed as the leading halves of two split-spread records. In Figure 2b, the differences in first-break traveltimes between common receivers for the two records are plotted versus distance. Zones B and D show that constant time differences ( $\delta t$ ) are obtained where first arrivals at common receivers in records  $sp_1$  and  $sp_2$  involve a common refractor. Zones A and C define regions where the first arrivals at common receivers do not involve common refractors. Zones B and D are defined as "difference windows" and the number of these windows determines directly the number of refractors present. In Figure 2a it is seen that the near boundaries of zones B, C, and D coincide with true crossover positions in the first-arrival data. An important feature of difference windows is that they are unaffected by either surface or refractor topography. Consequently, true crossover positions can be determined precisely.

Chun and Jacewitz (1981) also computed differential traveltimes between adjacent records, except that they applied a time correction to the first-break traveltimes, based on a "skewing velocity," to remove the moveout component.

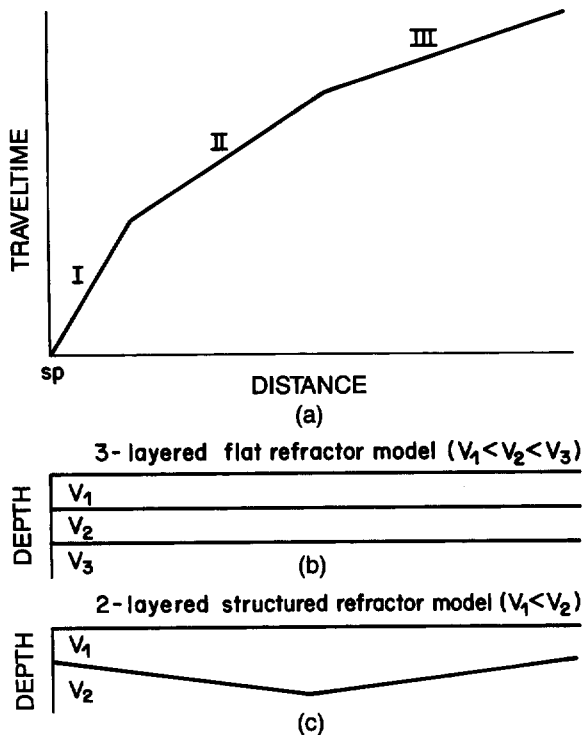


FIG. 1. (a) Traveltime-distance graph of first-break data showing three segments: (I), (II), and (III). Two possible interpretations of these data are shown as (b) a simple three-layered model and (c) a more complex, structured 2-layered model.

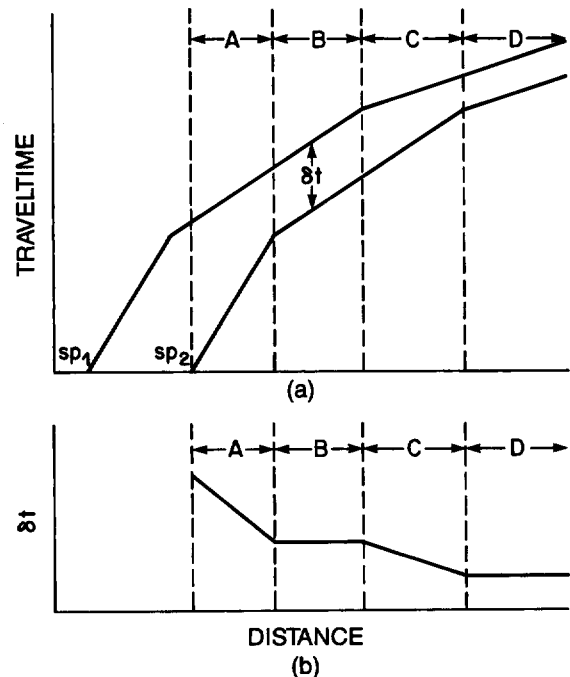


FIG. 2. Time-difference display (b) derived from two records shown in (a). Windows (B) and (D) with constant time differences ( $\delta t$ ) show offset ranges where the first arrivals from the two records are refracted from a common interface. These zones are defined to be "difference windows."

However, in the case of end-on records, errors in the skewing velocity result in increasing errors in the accumulated differential shot and receiver statics. Also, Chun and Jacewitz did not present a general case for multiple refractors.

**Shotpoint delay times**

Delay-time methods involve partitioning intercept times into shot and receiver delay times (Barry, 1967). This is easily accomplished for reciprocal records but is more difficult if only end-on records are available. In this case, one solution is to compute generalized half-intercept times (Palmer, 1980).

Figure 3a is a first-break travelttime-distance graph for three records with closely spaced shotpoints. Times  $t_{1,3}$  and  $t_{2,3}$  represent first-arrival traveltimes to a receiver at  $sp_3$  from  $sp_1$  and  $sp_2$ , respectively;  $t_{1,2}$  is the travelttime from  $sp_1$  to a receiver at  $sp_2$ . Distances  $x_{1,2}$ ,  $x_{2,3}$ , and  $x_{1,3}$  are the shotpoint separations, as shown in Figure 3a. The records need not necessarily be immediately adjacent to one

another but are selected to ensure that  $t_{1,3}$  and  $t_{2,3}$  lie within a common difference window. Assuming that the delay times ( $t_d$ ) for a shotpoint and receiver at a common location are equal, these traveltimes are given by

$$t_{1,3} = t_d(sp_1) + t_d(sp_3) + x_{1,3}/v_2 \tag{1}$$

and

$$t_{2,3} = t_d(sp_2) + t_d(sp_3) + x_{2,3}/v_2, \tag{2}$$

where  $v_2$  is the refractor velocity.

Let

$$\begin{aligned} \delta t_{1,2} &= t_{1,3} - t_{2,3} \\ &= t_d(sp_1) - t_d(sp_2) + x_{1,2}/v_2, \end{aligned} \tag{3}$$

since  $x_{1,2} = x_{1,3} - x_{2,3}$ .

Now

$$t_{1,2} = t_d(sp_1) + t_d(sp_2) + x_{1,2}/v_2. \tag{4}$$

Subtracting equation (3) from equation (4) yields

$$t_{1,2} - \delta t_{1,2} = 2t_d(sp_2); \tag{5}$$

i.e.,

$$t_d(sp_2) = [t_{1,2} - \delta t_{1,2}]/2,$$

thus determining the delay time at  $sp_2$ . The derivation of equation (5) is similar to that of the time term of Hawkins (1961) and the plus time of Hagedoorn (1959), except that in the case presented here, the common receiver lies to one side of both shotpoints. In the reciprocal methods, the common receiver must lie between the two shotpoints, requiring both forward and reverse spreads. Palmer (1980) defined the delay time in equation (5) as the "generalized half-intercept time."

In multifold surveys, the redundancy of first-break data allows several determinations of common-shotpoint delay times to be made. For example, Figure 3b shows five records with overlapping difference windows. Traveltimes  $t_{1,5}$ ,  $t_{2,5}$ , and  $t_{3,5}$  and the time differences  $\delta t_{1,5}$ ,  $\delta t_{2,5}$ , and  $\delta t_{3,5}$  can be used in equation (5) to calculate three independent values of the delay time at  $sp_5$ .

Delay times for deeper refractors can be computed in an identical manner by using difference windows which are successively further offset from the shotpoints. In the general case for difference window  $n$ , equation (5) can be expressed as

$$t_d(sp_k)_n = (1/j_{tot}) \sum_{j=1}^{j_{tot}} [(t_{j,k} - \delta t_{j,k})/2], \tag{6}$$

where  $j_{tot}$  is the number of records with overlapping difference windows at shotpoint  $sp_k$ . In this case, the delay time at  $sp_k$  for refractor  $n$  is also equivalent to

$$t_d(sp_k)_n = \sum_{m=1}^{n-1} [z_m(sp_k) \cos(i_{mn})/v_m], \tag{7}$$

where  $z_m(sp_k)$  is the thickness of layer  $m$  at  $sp_k$ ,  $v_m$  is the velocity of layer  $m$ , and  $i_{mn} = \sin^{-1}(v_m/v_n)$ . Rearrange-

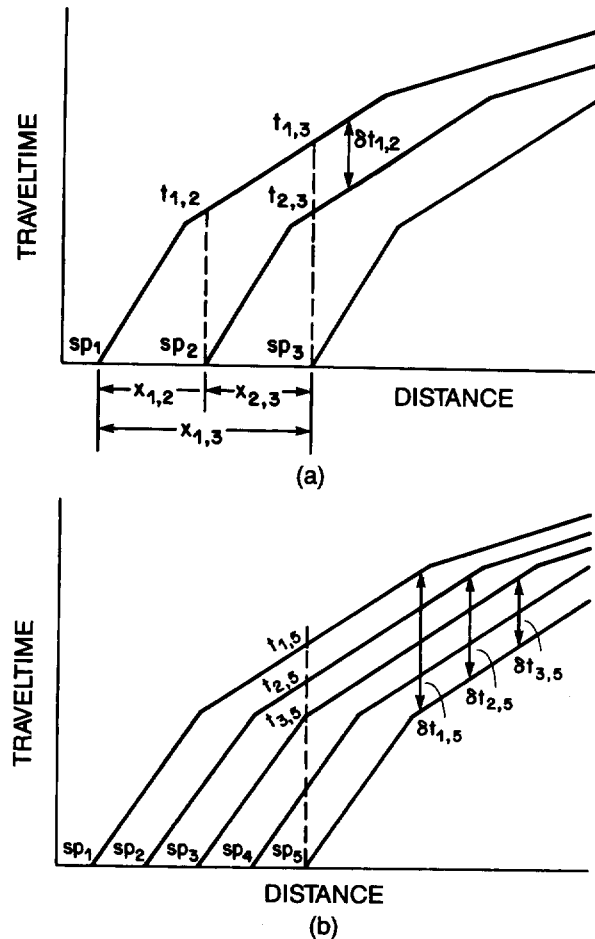


FIG. 3. (a) Definition of traveltimes, time differences, and source-receiver offsets for computation of the delay time at  $sp_2$ . (b) Extension of the method for the calculation of shot delay times from multifold surveys. In this example, three independent computations of the delay time at  $sp_5$  can be made.

ment of equation (7) allows  $z_m$  to be determined for all  $(n - 1)$  layers of the interpreted depth model.

**Refractor velocities**

Once the delay times at all shotpoints along the profile have been determined, the velocity of each refractor can be calculated by rearranging equations (1) or (2). For the case shown in Figure 3a,

$$v_2 = x_{1,3} / [t_{1,3} - t_d(\text{sp}_1) - t_d(\text{sp}_3)] \quad (8a)$$

or

$$v_2 = x_{2,3} / [t_{2,3} - t_d(\text{sp}_2) - t_d(\text{sp}_3)]. \quad (8b)$$

In the general case, the velocity of layer  $n$  is given by

$$v_n = (1/j_{\text{tot}}) \sum_{j=1}^{j_{\text{tot}}} \{x_{j,k} / [t_{j,k} - t_d(\text{sp}_j)_n - t_d(\text{sp}_k)_n]\}. \quad (9)$$

For each velocity determination,  $v_n$  is assigned to a location midway between the relevant shotpoint and the midpoint of the particular difference window. Again, the redundancy of first-break data available in multifold surveys enables many independent determinations of the refractor

velocities to be made at each position. If there are gaps along the seismic line where shots have had to be dropped, then there may be stations at which the refractor velocities have not been determined. In such cases, a velocity is assigned for each refractor by interpolation between values for that refractor at the closest adjacent stations.

**Remaining receiver delay times**

In land surveys, it is not usual to have a shotpoint at every surface station. Hence it is necessary to compute the delay times at the remaining receiver locations which do not coincide with shotpoints. The delay time  $t_d(r)$  at a receiver  $r$  within a difference window can be determined by rearranging equation (1),

$$t_d(r) = t_{1,r} - t_d(\text{sp}_1) - x_{1,r} / v_2. \quad (10)$$

The refractor velocity  $v_2$  is obtained from equation (8) for the particular source-receiver pair. In the general case,

$$t_d(r)_n = (1/j_{\text{tot}}) \sum_{j=1}^{j_{\text{tot}}} [t_{j,r} - t_d(\text{sp}_j)_n - x_{j,r} / v_n]. \quad (11)$$

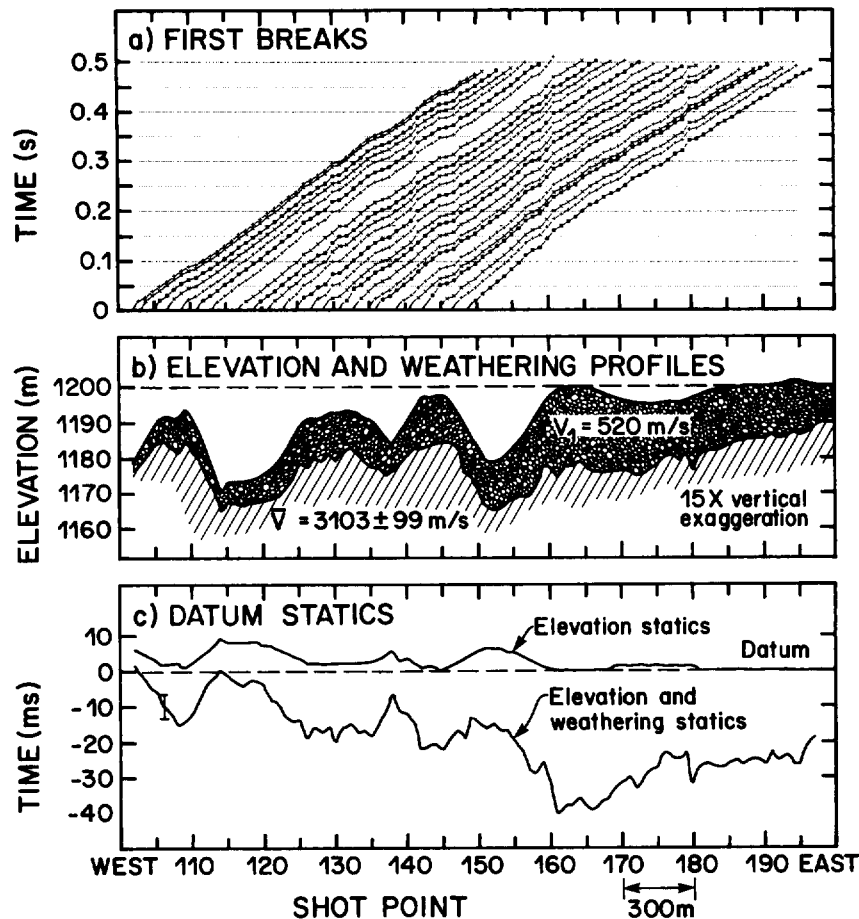


FIG. 4. (a) First breaks for line FS84-1. (b) Depth interpretation of weathering layer based on refraction analysis using the time-difference method. The dashed line at elevation 1200 m is the datum level for static corrections. (c) Profiles of the elevation and refraction static corrections along line FS84-1.

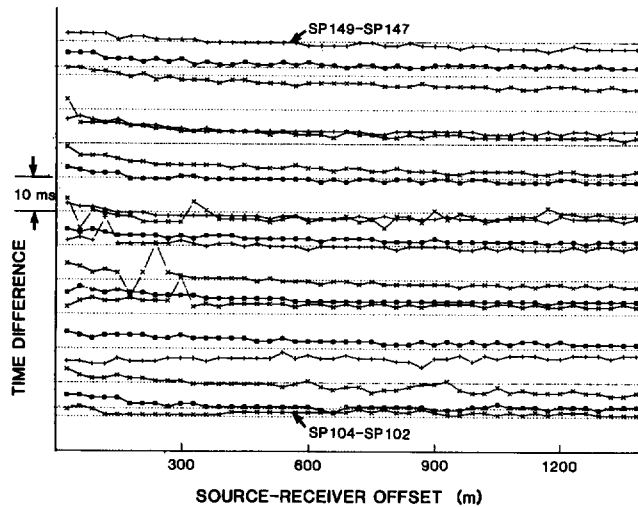


FIG. 5. Nested record-to-record time-difference curves of the first-break data shown in Figure 4a for a shotpoint separation of two group intervals.

Equations (10) and (11) can also be used to evaluate the delay times at the start and end of the line where shotpoints lie outside the minimum offset distance between the shotpoint and the difference window. Any remaining receiver delay times at stations near the ends of the seismic line are evaluated by interpolation.

#### Depth interpretation

The output of the above analysis is a complete suite of delay times and velocities for each refractor at each station along the seismic line. For surveys recorded with a split-spread geometry, completely independent data sets can be computed for the leading and trailing components of the spread.

Table 1. Shotpoint delay times for line FS84-1.

Shotpoint	Delay time (ms)	Standard Deviation (ms)	Number of samples
109	19.1	0.3	2
111	15.0	0.3	3
113	11.9	0.3	4
117	14.9	0.6	6
119	14.1	0.7	7
121	18.0	0.6	7
123	20.9	0.8	8
125	21.5	1.0	9
127	22.8	1.0	10
129	22.2	1.6	11
131	22.4	2.4	12
133	23.2	1.1	13
135	25.1	1.3	14
136	22.9	0.8	14
139	18.1	0.6	16
141	21.0	0.6	17
143	26.8	0.9	18
145	27.4	0.6	19
147	23.6	0.7	20
149	21.0	0.9	21

For converting delay times to depth, the velocity of the surface layer is required. This is achieved from uphole times for shothole surveys or from inverse slope analysis of the direct arrivals of traveltime-distance graphs for surveys using a surface source. The weathering velocity is relatively poorly controlled. However, in the Canadian Rocky Mountain foothills region, the computation of weathering static corrections from delay times is relatively insensitive to errors in the velocity of the surface layer, since the weathering layer is thin and has a large velocity contrast at its base.

Depth interpretation to each refractor is accomplished using equation (7) for each suite of difference-window delay times. Once the near-surface depth and velocity structure have been mapped, weathering and elevation static corrections to a desired datum are computed by velocity replacement.

#### EXAMPLE ANALYSIS

##### Data set

The refraction statics procedure is demonstrated using a seismic data set which was recorded in 1984 by the University of Calgary Geophysics Field School. The study area is 50 km northwest of Calgary, in southern Alberta, and is located on the eastern edge of the Rocky Mountain foothills. In this area, eastward-dipping underthrusting has formed the Triangle zone, which is a characteristic structural feature of the foreland margin of the Rocky Mountain thrust belt (Jones, 1982). Line FS84-1 was recorded with a 48-channel DFS III recording system using a group interval of 30 m, a near offset of 30 m, and an end-on shotpoint geometry with the shot placed at the western end of the spread. A dynamite source was used with a shothole depth of 18 m and a charge size of 1.0 kg.

Figure 4a is a plot of first-break traveltimes for the seismic records from line FS84-1. The data show short- and long-wavelength variations in traveltime due to changes in elevation and in weathering thickness along the line; an elevation profile is presented in Figure 4b. The first breaks were determined using an automatic picking routine, followed by careful manual checking and editing. As with all refraction interpretation methods, the accuracy of the final solution is dependent ultimately on the reliability of the first-break picks. Prior to the analysis, each record was given a positive time shift equal to its uphole time. This, in effect, converts from a shothole to a surface source.

##### Time differences

Time differences between records with a shotpoint separation of two group intervals are plotted in Figure 5. In this case, adjacent spreads overlap by 46 receivers. Time differences for traces nearest the shotpoints are displayed on the left of Figure 5; those for far traces are displayed on the right. Short-wavelength scatter in the data reflects residual picking errors. However, these are relatively isolated and are of small magnitude (less than 10 ms).

The data in Figure 5 were interpreted as a single difference

**Table 2. Refractor velocity determination.**

Location	Velocity (m/s)	Standard Deviation (m/s)	Number of samples
121	3086	65	17
122	3021	40	17
124	3053	66	16
127	3040	122	14
128	3053	122	13
130	3017	108	12
131	2981	80	11
133	3051	126	10
134	3093	100	9
136	3098	75	8
138	3078	55	6
139	3093	63	6
140	3275	130	5
141	3299	98	4
143	3252	150	3
145	3364	205	2

window between offsets of 6 and 48 group intervals (180 to 1440 m), indicating a simple, two-layered velocity structure. This interpretation is not obvious from the first-break plot (Figure 4a), which shows an apparent three-layered structure. However, this effect was found to be caused by surface and refractor topography, as well as by an increase in refractor velocity east of about shotpoint 140. At offset distances of less than six group intervals (180 m), the time differences decrease by about 5 ms, indicating that there is a velocity gradient at the top of the refractor. Beyond offsets of six group intervals, the very slight decrease in time difference (less than 3 ms) over the remaining spread length is indicative of a gradual but insignificant velocity increase with depth in the refractor. For the refraction analysis, the average time difference within the difference window was assumed to be constant. Although this induced a small error in the absolute depth determination, it had only a small effect on the computation of the static correction.

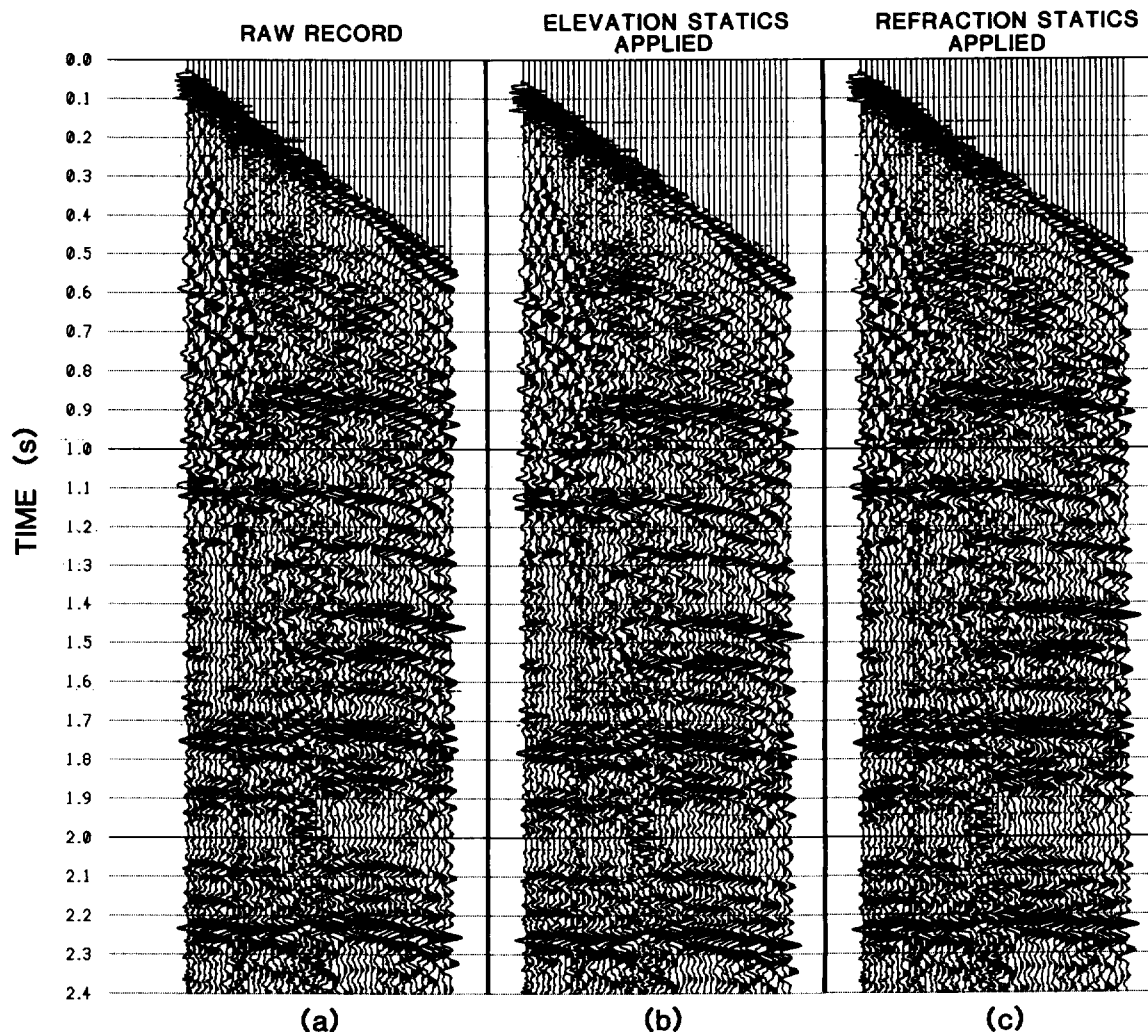


FIG. 6. (a) A raw shot record from line FS84-1, showing a weathering static anomaly over the center traces. The same record is shown in (b) with only elevation corrections applied, and in (c) after both elevation and weathering statics computed using the time-difference method have been applied.

## Results

Shotpoint delay times for all shot locations which satisfied the difference-window criterion were determined using equation (6); these data are given in Table 1. The redundancy in the data increases from west to east due to a greater number of overlapping spreads (Figure 4a). Confidence in the results was provided by a statistical analysis which showed standard deviations with a mean value of only 0.8 ms over the length of the line.

Table 2 contains the refractor velocities which were computed using equation (9). Based on 153 independent determinations, the average refractor velocity was found to be 3103 m/s with a standard deviation of 99 m/s. The data in Table 2 show a trend of increasing refractor velocity from about 3050 m/s at the western end of the line to about 3300 m/s at the eastern end. This velocity increase results in the apparent refractor crossovers in the first-break data (Figure 4a), as noted earlier.

The shotpoint delay time and velocity data contained in

Tables 1 and 2, respectively, were used in equation (11) to determine the delay times at all other receiver locations along the profile. A depth profile (Figure 4b) was then computed from the suite of delay times, using equation (7). The surface-layer velocity was calculated from uphole and direct-arrival times and averaged 520 m/s. This is a typical value for unconsolidated glacial sediments which cover the study area. The thickness of the weathering layer varies from 3 m at the western end of the line to over 20 m between stations 160 and 170 (Figure 4b).

## Static corrections

Static corrections at each surface station were computed to a datum of 1200 m by assuming a surface-layer velocity of 520 m/s. The replacement velocity used was 3103 m/s, the average refractor velocity determined from the first-break analysis. Computed static corrections ranged in magnitude from +1 ms to -40 ms and are plotted versus surface station in Figure 4c. The uncertainty in the static-correction values

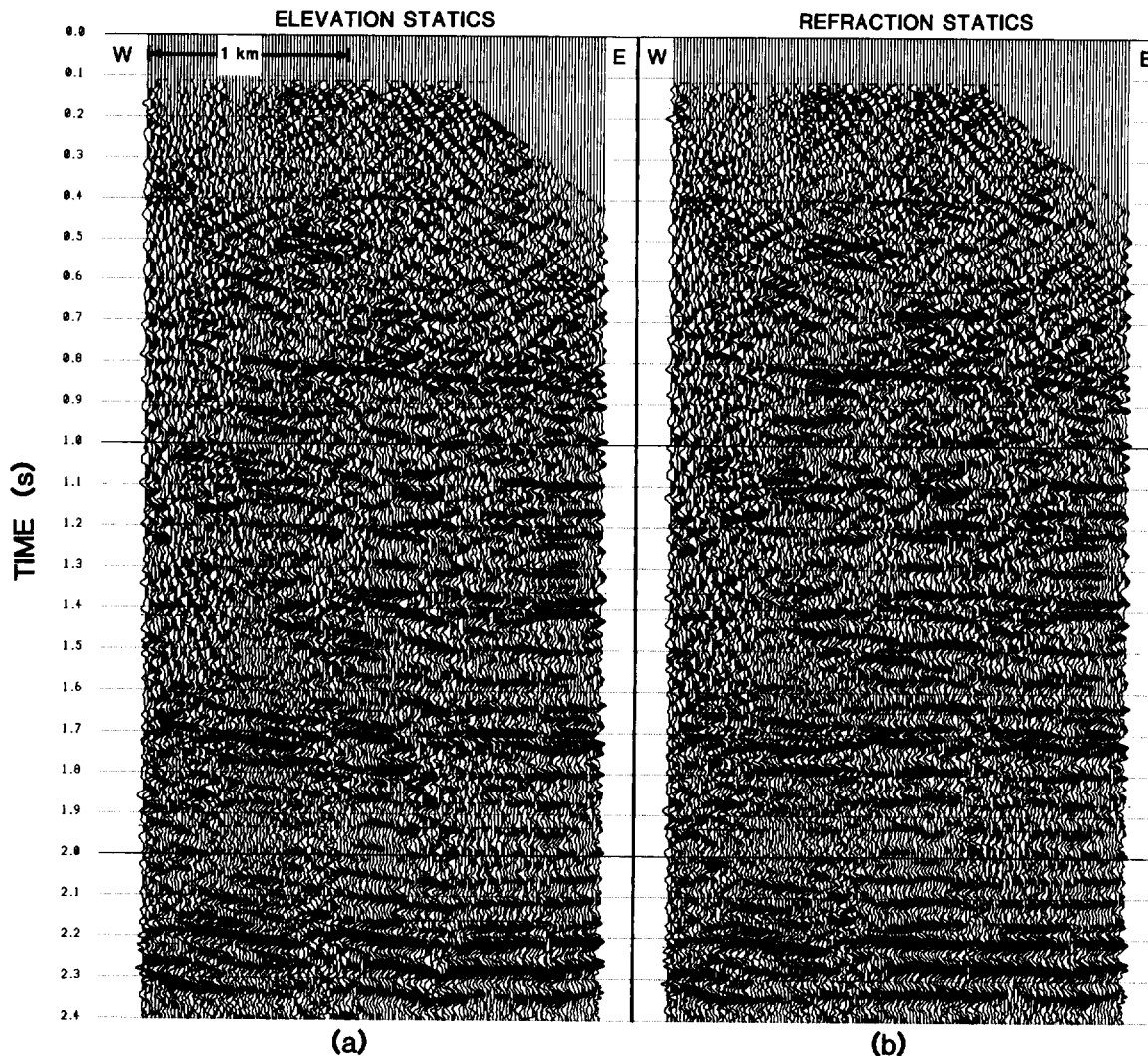


FIG. 7. Comparison of stacked sections from line FS84-1. (a) With elevation corrections only, (b) with elevation and weathering statics applied. No poststack processing was applied to either section.

is similar to that in the delay times. If a normal error distribution is assumed, then over the length of the seismic line, the 99 percent confidence level (three standard deviations) is  $\pm 2.4$  ms. The absolute values of the static corrections increase eastward in response to the increasing thickness of glacial overburden. For comparison, Figure 4c also shows elevation corrections only, computed to the same datum (1200 m) and using the same replacement velocity (3103 m/s). The range in values for the elevation corrections is less than 10 ms, indicating that the variation in weathering thickness along the seismic line has a much greater effect on reflection traveltimes than does the surface topography.

For each shot gather from line FS84-1, the shot and receiver statics were summed and applied to each trace. In Figure 6, a raw shot gather (Figure 6a) is compared with the same record after elevation corrections only (Figure 6b) and after full weathering static corrections (Figure 6c). An intermediate-wavelength weathering static anomaly evident in the center traces of the record was removed after application of weathering static corrections based on time differences. Elevation corrections alone failed to resolve the anomaly.

A further comparison is provided by the stacked sections of Figure 7. In Figure 7a, only elevation statics were applied, whereas full refraction statics to the same datum were applied to the data in Figure 7b. A poststack bulk shift of  $-25$  ms was applied to the section with elevation statics only (Figure 7a) to tie approximately the major reflection events with those in Figure 7b. With refraction statics applied, the coherency and continuity of reflections has improved considerably, and greater confidence could be placed on a structural interpretation.

### CONCLUSIONS

The following conclusions are drawn from this study:

(a) The time-difference method of refraction interpretation is a statistically powerful approach to the computation of weathering static corrections for reflection seismic data. It is a highly automated process which requires only limited manual input.

(b) Unlike most other techniques for refraction interpretation, the difference method does not require reciprocal records. This makes it highly applicable in marine surveys and in land recording where an end-on shot position is used.

(c) Refractor velocities are continuously mapped

and lateral variations in refractor velocities are accounted for in the computation of static corrections.

(d) Both short- and long-wavelength static anomalies can be resolved.

(e) In a test data set from the foothills of southern Alberta, weathering static anomalies were removed successfully from the data by corrections based on the time-difference method. Corrections of up to 40 ms were computed, with a maximum uncertainty of  $\pm 2.4$  ms.

(f) The limitation of the method is that there must be a reasonably regular spacing of shotpoints. If a gap greater than about one-half of a spread length occurs, then records have to be "phantomed" within the gap.

### ACKNOWLEDGMENTS

Data used in this study were collected by students and staff of the Department of Geology and Geophysics, The University of Calgary, who participated in the 1984 Geophysics Field School. Funding for this study was provided by a grant from the Natural Sciences and Engineering Research Council of Canada. Useful criticism was provided by anonymous reviewers.

### REFERENCES

- Barry, K. M., 1967, Delay time and its application to refraction profile interpretation, *in* Musgrave, A. W., Ed., *Seismic refraction prospecting*: Soc. Expl. Geophys., 348-361.
- Chun, J. H., and Jacewitz, C. A., 1981, The first arrival time surface and estimation of statics: presented at the 51st Ann. Internat. Mtg., Soc. Expl. Geophys.
- Cunningham, A. B., 1974, Refraction data from single-ended refraction profiles: *Geophysics*, **39**, 292-301.
- Gardner, L. W., 1939, An areal plan of mapping subsurface structure by refraction shooting: *Geophysics*, **4**, 247-259.
- Gardner, L. W., 1967, Refraction seismograph profile interpretation, *in* Musgrave, A. W., Ed., *Seismic refraction prospecting*: Soc. Expl. Geophys., 338-347.
- Hagedoorn, J. G., 1959, The plus-minus method of interpreting seismic refraction sections: *Geophys. Prosp.*, **7**, 158-182.
- Hampson, D., and Russell, B., 1984, First break interpretation using generalized linear inversion: *J. Can. Soc. Expl. Geophys.*, **20**, 40-54.
- Hawkins, L. V., 1961, The reciprocal method of routine shallow seismic refraction investigations: *Geophysics*, **26**, 806-819.
- Hollingshead, G. W., and Slater, R. R., 1979, A novel method of deriving weathering statics from first arrival refractions: Presented at the 49th Ann. Internat. Mtg., Soc. Expl. Geophys.
- Jones, P. B., 1982, Oil and gas beneath east-dipping underthrust faults in the Alberta foothills, *in* Powers, R. B., Ed., *Studies of the Cordilleran thrust belt*: Rocky Mountain Assn. of Geol., 61-74.
- Palmer, D., 1980, The generalized reciprocal method of seismic refraction interpretation: Soc. Expl. Geophys.
- Sheriff, R. E., 1984, *Encyclopedic dictionary of exploration geophysics*, 2nd ed.: Soc. Expl. Geophys.